CLINICAL REPORT

AMERICAN JOURNAL OF medical genetics PART A

Vertebral Fusion in a Patient With Supernumerary-der(22)t(11;22) Syndrome

Mitsuo Toyoshima,[1]* Chihiro Yonee,[1] Yoshihiro Maegaki,[2] Toshiyuki Yamamoto,[3] Keiko Shimojima,[3] Shinsuke Maruyama,[1] and Yoshifumi Kawano[1]

[1]Department of Pediatrics, Graduate School of Medical and Dental Sciences, Kagoshima University, Kagoshima City, Kagoshima, Japan

[2]Division of Child Neurology, Institute of Neurological Science, Tottori University Faculty of Medicine, Yonago City, Tottori, Japan

[3]International Research and Educational Institute for Integrated Medical Sciences (IREIIMS), Tokyo Women's Medical University, Tokyo, Japan

Received 22 July 2008; Accepted 18 January 2009

A patient with a 47,XX,+der(22)t(11;22)(q23.3;q11.2) karyotype exhibited brisk tendon reflex and Babinski sign with suggested pyramidal sign. A three-dimensional computed tomographic reconstruction revealed a T1-T2 vertebral fusion without hemivertebrae. Sagittal magnetic resonance imaging revealed degenerative disk changes, mild disk herniation, and mild spinal cord compression. Congenital vertebral fusion may be one of the anomalies in supernumerary-der(22)t(11;22) syndrome. Once clinical diagnosis of this chromosome aberration is established, radiologic evaluation of vertebrae and spinal neuroimaging should be performed. © 2009 Wiley-Liss, Inc.

Key words: supernumerary-der(22)t(11;22) syndrome; Emanuel syndrome; congenital vertebral fusion; *TBX1*

How to Cite this Article:
Toyoshima M, Yonee C, Maegaki Y, Yamamoto T, Shimojima K, Maruyama S, Kawano Y. 2009. Vertebral fusion in a patient with supernumerary-der(22)t(11;22) syndrome.
Am J Med Genet Part A 149A:1722–1726.

INTRODUCTION

The balanced t(11;22) translocations are the most common recurrent non-Robertsonian constitutional translocation in humans. 47,XX (or XY),+der(22)t(11;22)(q23.3;q11.2) karyotype, supernumerary-der(22)t(11;22) syndrome or Emanuel syndrome [OMIM 609029], is the result of a 3:1 meiotic disjunction from the parental t(11;22) and often leads to spontaneous abortions [Zackai and Emanuel, 1980]. Although major manifestations include mental retardation, microcephaly, characteristic facial features, cleft palate, preauricular skin tags and sinuses, congenital heart defects, congenital dislocation of the hips, and anal atresia [Fraccaro et al., 1980; Zackai and Emanuel, 1980; Shinzel et al., 1981], congenital vertebral fusion has rarely been reported in the literature. Several candidate genes putatively responsible for congenital vertebral malformations have been reported, the mechanisms of faulty segmentation of the vertebrae are not well elucidated. Congenital vertebral fusion is a relatively common malformation, and therefore it is important to keep in mind that vertebral fusion possess a risk for spinal cord injury at minor trauma.

We describe here a patient with thoracic vertebral fusion and spinal cord compression associated with 47,XX,+der(22)t(11;22)(q23.3;q11.2) karyotype resulting from maternal translocation t(11;22).

CLINICAL REPORT

This Japanese female patient was the first child of healthy parents. Her mother had previously had five spontaneous abortions. The mother was 39 years and the father was 41 years old at the time of her birth. She was born by cesarean section because of late primipara at 39 weeks gestation. Her birth weight was 2,500 g. Birth length and occipitofrontal circumference were not reported. At birth, she had anal atresia, atrial septal defect, cleft palate, and bilateral preauricular skin tags and a pronounced dimple, for which she underwent surgery. Nasogastric tube feeding was required due to feeding difficulties until 3 months of age. At 3 months, bilateral congenital dislocation of the hips was diagnosed and treated orthopedically. Her development was severely retarded since early infancy. From the age of 6 months, she received special training for developmental delay. She was able to roll over at 10 months of age, and to sit alone at 3 years of age. Her global development quotient (DQ) was 20 at 3.3 years of age. She started to walk without support at 4 years of age. Her DQ was 17 at the age of 5.2 years. There was no past history of traffic accident, abrupt onset of motor paralysis, surgical operation of spine, or rheumatic disease.

*Correspondence to:
Mitsuo Toyoshima, Department of Pediatrics, Graduate School of Medical and Dental Sciences, Kagoshima University, 8-35-1 Sakuragaoka, Kagoshima City, Kagoshima 890-8520, Japan.
E-mail: toyoshim@m2.kufm.kagoshima-u.ac.jp
Published online 7 April 2009 in Wiley InterScience (www.interscience.wiley.com)
DOI 10.1002/ajmg.a.32762

© 2009 Wiley-Liss, Inc.

At 16 years of age, she was referred to our hospital for epileptic seizure. Her height was 149 cm (−1.7 SD), weight 42.9 kg (−1.3 SD) and occipitofrontal circumference 52.5 cm (−2.0 SD). She was able to walk unstably but could not speak any words. Physical examination identified a distinctive pattern of dysmorphic features, including a broad nose, prominent lower lip, bilateral low set ears, kyphoscoliosis, Sprengel deformity, supranumerary digital flexion creases with normal joint anatomy in all of the digits (Fig. 1), mild right upper limb micromelia (Fig. 1), and persistent papillary membrane. Because no epibulbar dermoid was noted, Goldenhar syndrome was negative. Neurological examinations revealed profound mental retardation, brisk tendon reflex more prominent in the lower extremities than the upper extremities, Babinski sign, negative jaw reflex, stereotypic movements with arms and hands, mixed deafness, and alternating strabismus. She did not display meningeal sign, involuntary movements, or an impairment of the cranial nerves.

The following laboratory tests were normal: complete blood cell count, blood chemistry, coagulation and fibrinolysis tests, blood glucose, blood lactate, blood immunoglobulin, autoantibodies, complement, rheumatoid factor and urinalysis. Cytogenetic studies of a blood sample revealed a 47,XX,+der(22)t(11;22)(q23.3;q11.2) karyotype. The maternal karyotype was identified as 46,XX,t(11;22)(q23.3;q11.2).

The brain computed tomography findings were almost normal except for a mild widening of the lateral ventricles. An abdominal computed tomography revealed no abnormalities, including renal anomalies. A three-dimensional computed tomographic reconstruction revealed a T1-T2 vertebral fusion without hemivertebrae (Fig. 2A,B). Sagittal magnetic resonance imaging (fluid-attenuated inversion recovery images, 2960/88: [TR/TE]) revealed degenerative disk change, mild disk herniations, and mild spinal cord compression at C4-C5 and C5-C6 levels (Fig. 2C). Based on the past history, physical examinations, and laboratory findings, the vertebral fusion was considered to be congenital.

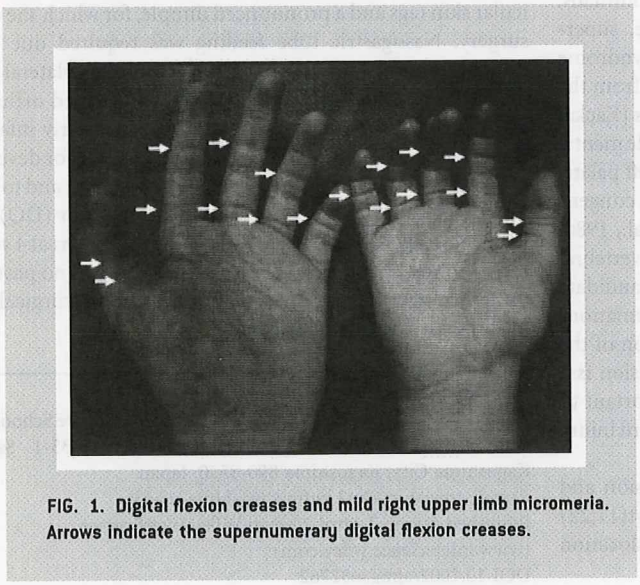

FIG. 1. Digital flexion creases and mild right upper limb micromeria. Arrows indicate the supernumerary digital flexion creases.

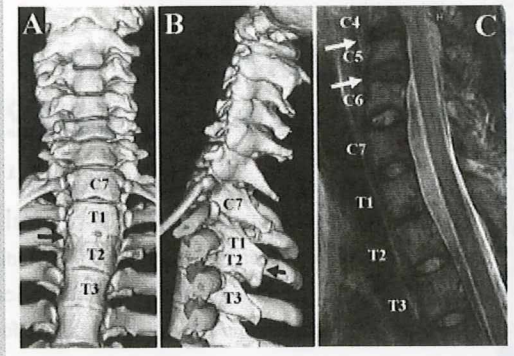

FIG. 2. Neuroimaging of the vertebrae and spinal cord. A: Frontal view and (B) lateral view. Three-dimensional reconstruction of computed tomography shows congenital fusion of the vertebral bodies (A) and spinous process (B) of T1-T2 (arrows). C: Sagittal MRI (2960/88 [TR/TE]) shows degenerative and bulging disk changes, and mild spinal cord compression at C4-C5 and C5-C6 levels (arrows).

Interictal electroencephalogram revealed spike waves in a right central region. Epileptic seizures stopped upon carbamazepine treatment.

Methods of Laboratory Examination

Array-based comparative genomic hybridization (aCGH) analyses were performed using the Human Genome CGH Microarray 105A chip (Agilent Technologies, Santa Clara, CA) as described elsewhere [Toruner et al., 2007]. Genomic copy number aberrations were determined using the ADM-II algorithm in CGH Analytics version 3.5 (Agilent Technologies).

Fluorescent in situ hybridization (FISH) analysis was performed using metaphase or prometaphase chromosomes prepared from phytohemagglutinin-stimulated peripheral blood lymphocytes using standard techniques. The BAC clones RP11-316L10 (18,073,141//18,286,591) and RP11-927B11 (45,858,870//46,056,130) mapping to the region 22q11.21 and 22q13.31, respectively, were selected from build 2006. Two-color FISH analyses using BAC clones as probes were performed as described [Shimokawa et al., 2004].

RESULTS

aCGH analysis for the presenting patient confirmed gains of genomic copy number on the chromosomal regions of 22q11.21 and 11q23.3-q25 (Fig. 3a,b), which indicates the additional derivative chromosome t(11;22). aCGH analytics showed both chromosomal break points on 22q11.21 (18.9-Mb) and 11q23.3 (116.2-Mb), respectively (Fig. 3c,d). They were the standard breakpoints of supernumerary-der(22)t(11;22) syndrome. FISH analysis

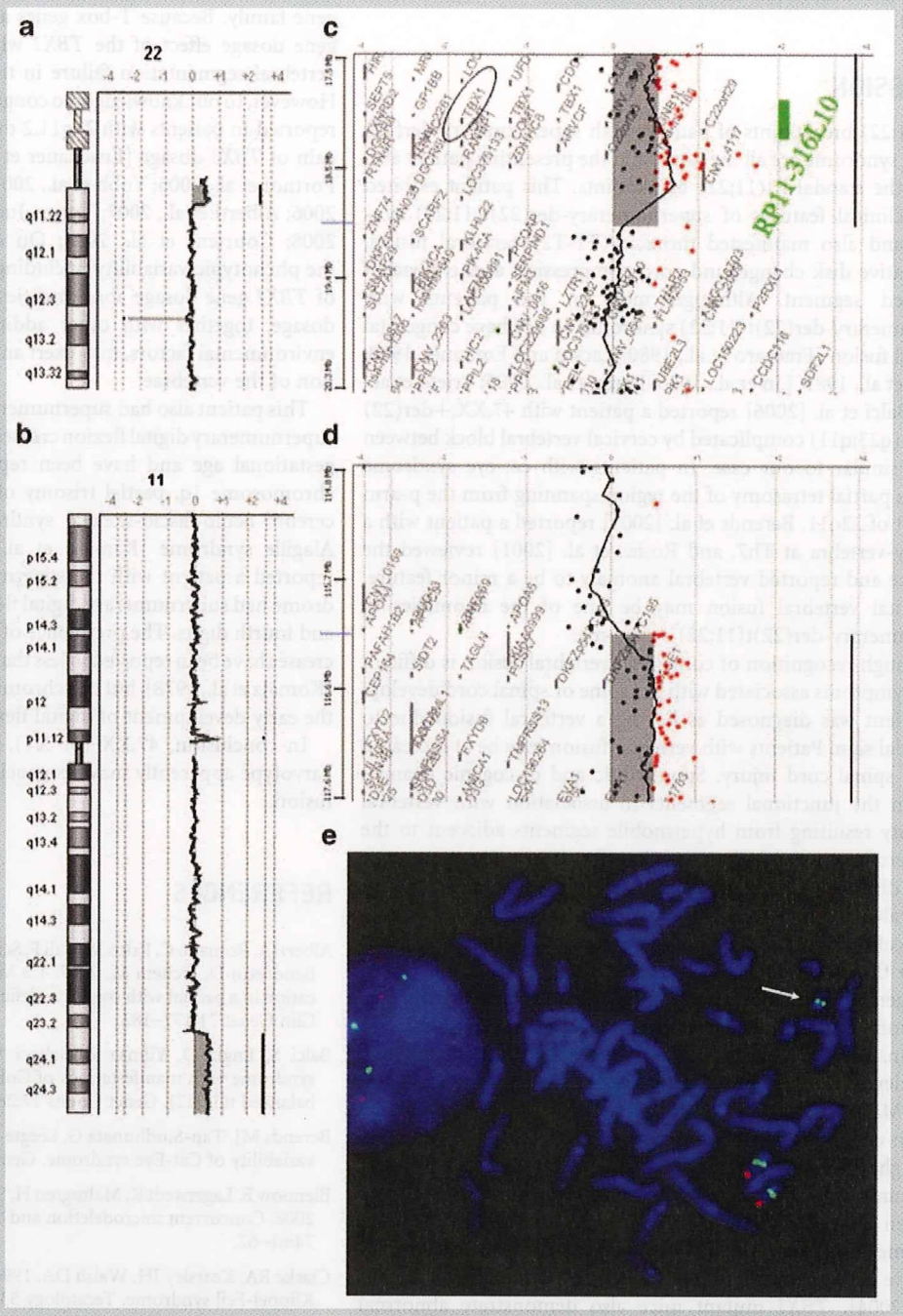

FIG. 3. aCGH analysis shown by CGH Analytics version 3.5, with a weighted moving average of 0.5-Mb. On both chromosome 22 and 11, there are regions of genomic copy number gains in chromosome view (a,b). The regions of break points are expanded in gene view (c,d). The region of *TBX1*, highlighted by circle, indicates genomic copy number gain. A green rectangle indicates the location of the FISH probe used (RP11-316L10) covering *TBX1*. The vertical axis and each dot mean the physical position with known genes and the position of an individual probe, respectively. On the horizontal axis, plus and minus signs indicate the log2 ratio of gain and loss of genomic copy number, respectively. Two-color FISH analysis using a combination of the BAC clones RP11-316L10 (green) and RP11-927B11 (red) as probes, which locate on 22q11.21 and 22q13.31, respectively (e). An arrow indicates a derivative chromosome 22 in which green signal is visible but no red signal. [Color figure can be viewed in the online issue, which is available at www.interscience.wiley.com.]

confirmed the existence of *TBX1* on the derivative chromosome (Fig. 3e).

DISCUSSION

The t(11;22) breakpoints of patients with supernumerary-der(22)t(11;22) syndrome are all the same, and the presenting patient also carried the standard t(11;22) breakpoints. This patient exibited typical clinical features of supernumerary-der(22)t(11;22) syndrome and also manifested thoracic (T1-T2) vertebral fusion, degenerative disk change, and cord compression at the adjacent non-fused segment. Although most of the patients with supernumerary-der(22)t(11;22) syndrome do not have congenital vertebral fusion [Fraccaro et al., 1980; Zackai and Emanuel, 1980; Shinzel et al., 1981; Lin et al., 1986; Drum et al., 2005; Prieto et al., 2007], Balci et al. [2006] reported a patient with 47,XX,+der(22)t(11;22)(q23;q11) complicated by cervical vertebral block between C1-C2, similar to our case. In patients with cat-eye syndrome having a partial tetrasomy of the region spanning from the p-arm to a part of 22q11, Berends et al. [2001] reported a patient with a butterfly-vertebra at Th7, and Rosias et al. [2001] reviewed the literature and reported vertebral anomaly to be a minor feature. Congenital vertebral fusion may be one of the anomalies in supernumerary-der(22)t(11;22) syndrome.

Although recognition of congenital vertebral fusion is difficult unless symptoms associated with the spine or spinal cord develop, our patient was diagnosed as having a vertebral fusion due to pyramidal sign. Patients with vertebral fusion may be at increased risk for spinal cord injury. Spondylotic and discogenic changes occur in the junctional segments in association with vertebral instability resulting from hypermobile segments adjacent to the fused vertebrae [Mac Millan and Stauffer, 1991]. Therefore once clinical diagnosis of this syndrome is established, vertebral radiologic evaluation and spinal neuroimaging should be performed. Identification of vertebral fusions helps provide appropriate guidance for the prevention of spinal cord injury.

Congenital fusions of the vertebrae result from the faulty segmentation of the somites between the 3rd and 8th weeks of gestation. Several regulatory genes which play a significant role in the development of the axial skeleton, such as *PAX1*, *SGM1*, *DLL3*, *MESP2*, *LNFG*, *TBX1*, have been reported as candidate genes in congenital vertebral malformation [Clarke et al., 1996; McGaughran et al., 2003; Yagi et al., 2003; Giampietro et al., 2005; Turnpenny et al., 2007]. *TBX1* maps to chromosome 22q11.2, and has been suggested as a candidate gene for 22q11.2 deletion syndrome [Yagi et al., 2003]. Many congenital vertebral abnormalities have been reported in 22q11.2 deletion syndrome [Ricchetti et al., 2004]. *TBX1* mutant mice also demonstrate abnormal vertebrae [Jerome and Papaioannou, 2001; Lindsay et al., 2001] and mice carrying extra copies of *TBX1* have been found to display the full spectrum of malformations of the 22q11.2-deletion syndrome [Liao et al., 2004].

The supernumerary-der(22)t(11;22) syndrome is trisomic for both the 11q23-qter and the 22pter-q11 region. The trisomic region on chromosome 22 overlaps the deletion region in 22q11.2 deletion syndrome [Funke et al., 1999]. The results of aCGH and FISH analysis in our patient confirmed supernumerary-der(22)t(11;22) syndrome with trisomy of *TBX1*. *TBX1* is a member of the T-box gene family. Because T-box genes are dose-sensitive, it may be a gene dosage effect of the *TBX1* which results in the congenital vertebral segmentation failure in this partial trisomy syndrome. However, to our knowledge, no congenital vertebral fusion has been reported in patients with 22q11.2 duplication syndrome having a gain of *TBX1* dosage [Ensenauer et al., 2003; Hassed et al., 2004; Portnoï et al., 2005; Yobb et al., 2005; de La Rochebrochard et al., 2006; Alberti et al., 2007; Torres-Juan et al., 2007; Blennow et al., 2008; Courtens et al., 2008; Ou et al., 2008]. The origins of the phenotypic variability, including vertebral anomalies, in cases of *TBX1* gene dosage abnormalities are unknown. Altered *TBX1* dosage, together with other additional genetic, epigenetic, or environmental factors, may exert an affect on the faulty segmentation of the vertebrae.

This patient also had supernumerary digital flexion creases. The supernumerary digital flexion creases appear between 7 and 9 weeks gestational age and have been reported in partial deletions of chromosome 1q, partial trisomy of 14q, partial trisomy of 13q, cerebro-oculo-fascio-skeletal syndrome, sickle cell disease, and Alagille syndrome [Kamath et al., 2003]. Nakai et al. [1979] reported a patient with the supernumerary-der(22)t(11;22) syndrome had supernumerary digital flexion creases on the right third and fourth digits. The prevalence of supernumerary digital flexion creases have been reported in less than 1% of the general population [Komatz et al., 1978], but this chromosomal abnormality may affect the early development of digital flexion creases.

In conclusion, 47,XX (or XY),+der(22)t(11;22)(q23.3;q11.2) karyotype apparently may be associated with congenital vertebral fusion.

REFERENCES

Alberti A, Romano C, Falco M, Calì F, Schinocca P, Galesi O, Spalletta A, Di Benedetto D, Fichera M. 2007. 1.5 Mb de novo 22q11.21 microduplication in a patient with cognitive deficits and dysmorphic facial features. Clin Genet 71:177–182.

Balci S, Engiz O, Yilmaz Z, Baltaci V. 2006. Partial trisomy (11;22) syndrome with manifestations of Goldenhar sequence due to maternal balanced t(11;22). Genet Couns 17:281–289.

Berends MJ, Tan-Sindhunata G, Leegte B, van Essen AJ. 2001. Phenotypic variability of Cat-Eye syndrome. Genet Couns 12:23–34.

Blennow E, Lagerstedt K, Malmgren H, Sahlén S, Schoumans J, Anderlid B. 2008. Concurrent microdeletion and duplication of 22q11.2. Clin Genet 74:61–67.

Clarke RA, Kearsley JH, Walsh DA. 1996. Patterned expression in familial Klippel-Feil syndrome. Teratology 53:152–157.

Courtens W, Schramme I, Laridon A. 2008. Microduplication 22q11.2: A benign polymorphism or a syndrome with a very large clinical variability and reduced penetrance?—Report of two families. Am J Med Genet Part A 146A:758–763.

de La Rochebrochard C, Joly-Hélas G, Goldenberg A, Durand I, Laquerrière A, Ickowicz V, Sauier-Veber P, Eurin D, Moirot H, Diguet A, de Kergal F, Tiercin C, Mace B, Marpeau L, Frebourg T. 2006. The intrafamilial variability of the 22q11.2 microduplication encompasses a spectrum from minor cognitive deficits to severe congenital anomalies. Am J Med Genet Part A 140A:1608–1613.

Drum ET, Herlich A, Levine B, Mayhew JF. 2005. Anesthesia in a patient with chromosome 11;22 translocation: a case report and literature review. Paediatr Anaesth 15:985–987.

Ensenauer RE, Adeyinka A, Flynn HC, Michels VV, Lindor NM, Dawson DB, Thorland EC, Lorentz CP, Goldstein JL, Mc Donald MT, Smith WE, Simon-Fayard E, Alexander AA, Kulharya AS, Ketterling RP, Clark RD, Jalal SM. 2003. Microduplication 22q11.2, an emerging syndrome: Clinical, cytogenetic, and molecular analysis of thirteen patients. Am J Hum Genet 73:1027–1040.

Fraccaro M, Lindsten J, Ford CE, Iselius L. 1980. The 11q;22q translocation: A European collaborative analysis of 43 cases. Hum Genet 56:21–51.

Funke B, Edelmann L, McCain N, Pandita RK, Ferreira J, Merscher S, Zohouri M, Cannizzaro L, Shanske A, Morrow BE. 1999. Der(22) syndrome and velo-cardio-facial syndrome/DiGeorge syndrome share a 1.5-Mb region of overlap on chromosome 22q11. Am J Hum Genet 64:747–758.

Giampietro PF, Raggio CL, Reynolds CE, Shukla SK, McPherson E, Ghebranious N, Jacobsen FS, Kumar V, Faciszewski T, Pauli RM, Rasmussen K, Burmester JK, Zaleski C, Merchant S, David D, Weber JL, Glurich I, Blank RD. 2005. An analysis of *PAX1* in the development of vertebral malformations. Clin Genet 68:448–453.

Hassed SJ, Hopcus-Niccum D, Zhang L, Li S, Mulvihill JJ. 2004. A new genomic duplication syndrome complementary to the velocardiofacial (22q11 deletion) syndrome. Clin Genet 65:400–404.

Jerome LA, Papaioannou VE. 2001. DiGeorge syndrome phenotype in mice mutant for the T-box gene, Tbx1. Nature Genet 27:286–291.

Kamath BM, Loomes KM, Oakey RJ, Krantz ID. 2003. Supernumerary digital flexion creases: An additional clinical manifestation of Alagille syndrome. Am J Med Genet 112:171–175.

Komatz Y, Daijo K, Yoshida O. 1978. Extra interphalangeal transverse creases of the little finger. Jinrui Idengaku Zasshi 23:31–36.

Liao J, Kochilas L, Nowotschin S, Arnold JS, Aggarwal VS, Epstein JA, Brown MC, Adams J, Morrow BE. 2004. Full spectrum of malformations in velo-cardio-facial syndrome/DiGeorge syndrome mouse models by altering Tbx1 dosage. Hum Mol Genet 13:1577–1585.

Lin AE, Bernar J, Chin AJ, Sparkes RS, Emanuel BS, Zackai EH. 1986. Congenital heart disease in supernumerary der(22),t(11;22) syndrome. Clin Genet 29:269–275.

Lindsay EA, Vitelli F, Su H, Morishima M, Huynh T, Pramparo T, Jurecic V, Ogunrinu G, Sutherland HF, Scambler PJ, Bradley A, Baldini A. 2001. TBX1 haploinsufficieny in the DiGeorge syndrome region causes aortic arch defects in mice. Nature 410:97–101.

McGaughran JM, Oates A, Donnai D, Read AP, Tassabehji M. 2003. Mutations in PAX1 may be associated with Klippel-Feil syndrome. Eur J Hum Genet 11:468–474.

Mac Millan M, Stauffer ES. 1991. Traumatic instability in the previously fused cervical spine. J Spinal Disord 4:449–454.

Nakai H, Yamamoto Y, Kuroki Y. 1979. Partial trisomy of 11 and 22 due to familial translocation t(11;22)(q23;q11), inherited in three generations. Hum Genet 51:349–355.

Ou Z, Berg JS, Yonath H, Enciso VB, Miller DT, Picker J, Lenzi T, Keegan CE, Sutton VR, Belmont J, Chinault AC, Lupski JR, Cheung SW, Roeder E, Patel A. 2008. Microduplications of 22q11.2 are frequently inherited and are associated with variable phenotypes. Genet Med 10:267–277.

Portnoï MF, Lebas F, Gruchy N, Ardalan A, Biran-Mucignat V, Malan V, Finkel L, Roger G, Ducrocq S, Gold F, Taillemite JL, Marlin S. 2005. 22q11.2 duplication syndrome: Two new familial cases with some overlapping features with DiGeorge/velocardiofacial syndromes. Am J Med Genet Part A 137A:47–51.

Prieto JC, Garcia NM, Elder FF, Zinn AR, Baker LA. 2007. Phenotypic expansion of the supernumerary derivative (22) chromosome syndrome: VACTERL and Hirschsprung's disease. J Pediatr Surg 42:1928–1932.

Ricchetti ET, States L, Hosalkar HS, Tamai J, Maisenbacher M, McDonald-McGinn DM, Zackai EH, Drummond DS. 2004. Radiographic study of the upper cervical spine in the 22q11.2 deletion syndrome. J Bone Joint Surg Am 86:1751–1760.

Rosias PR, Sijstermans JM, Theunissen PM, Pulles-Heintzberger CF, De Die-Smulders CE, Engelen JJ, Van Der Meer SB. 2001. Phenotypic variability of the cat eye syndrome. Case report and review of the literature. Genet Couns 12:273–282.

Shinzel A, Schmid W, Auf der Maur P, Moser H, Degenhardt KH, Geisler M, Grubisic A. 1981. Incomplete trisomy 22. I. Familial 11/22 translocation with 3:1 meiotic disjunction. Delineation of a common clinical picture and report of nine new cases from six families. Hum Genet 56:249–262.

Shimokawa O, Kurosawa K, Ida T, Harada N, Kondoh T, Miyake N, Yoshiura K, Kishino T, Ohta T, Niikawa N, Matsumoto N. 2004. Molecular characterization of inv dup del(8p): Analysis of five cases. Am J Med Genet Part A 128A:133–137.

Torres-Juan L, Rosell J, Morla M, Vidal-Pou C, García-Algas F, de la Fuente MA, Juan M, Tubau A, Bachiller D, Bernues M, Perez-Granero A, Govea N, Busquets X, Heine-Suñer D. 2007. Mutations in TBX1 genocopy the 22q11.2 deletion and duplication syndromes: A new susceptibility factor for mental retardation. Eur J Hum Genet 15:658–663.

Toruner GA, Streck DL, Schwalb MN, Dermody JJ. 2007. An oligonucleotide based array-CGH system for detection of genome wide copy number changes including subtelomeric regions for genetic evaluation of mental retardation. Am J Med Genet Part A 143A:824–829.

Turnpenny PD, Alman B, Cornier AS, Giampietro PF, Offiah A, Tassy O, Pourquié O, Kusumi K, Dunwoodie S. 2007. Abnormal vertebral segmentation and the notch signaling pathway in man. Dev Dyn 236: 1456–1474.

Yagi H, Furutani Y, Hamada H, Sasaki T, Asakawa S, Minoshima S, Ichida F, Joo K, Kimura M, Imamura S, Kamatani N, Momma K, Takao A, Nakazawa M, Shimizu N, Matsuoka R. 2003. Role of TBX1 in human del22q11.2 syndrome. Lancet 362:1366–1373.

Yobb TM, Somerville MJ, Willatt L, Firth HV, Harrison K, MacKenzie J, Gallo N, Morrow BE, Shaffer LG, Babcock M, Chernos J, Bernier F, Sprysak K, Christiansen J, Haase S, Elyas B, Lilley M, Bamforth S, McDermid HE. 2005. Microduplication and triplication of 22q11.2: A highly variable syndrome. Am J Hum Genet 76:865–876.

Zackai EH, Emanuel BS. 1980. Site-specific reciprocal translocation, t(11;22) (q23;q11), in several unrelated families with 3:1 meiotic disjunction. Am J Med Genet 7:507–521.

Maternal Uniparental Disomy 14 Syndrome Demonstrates Prader-Willi Syndrome-Like Phenotype

Kana Hosoki, MS, Masayo Kagami, MD, PhD, Touju Tanaka, MD, PhD, Masaya Kubota, MD, PhD, Kenji Kurosawa, MD, PhD, Mitsuhiro Kato, MD, PhD, Kimiaki Uetake, MD, Jun Tohyama, MD, PhD, Tsutomu Ogata, MD, PhD, and Shinji Saitoh, MD, PhD

Objective To delineate the significance of maternal uniparental disomy 14 (upd(14)mat) and related disorders in patients with a Prader-Willi syndrome (PWS)–like phenotype.

Study design We examined 78 patients with PWS-like phenotype who lacked molecular defects for PWS. The *MEG3* methylation test followed by microsatellite polymorphism analysis of chromosome 14 was performed to detect upd(14)mat or other related abnormalities affecting the 14q32.2-imprinted region.

Results We identified 4 patients with upd(14)mat and 1 patient with an epimutation in the 14q32.2 imprinted region. Of the 4 patients with upd(14)mat, 3 had full upd(14)mat and 1 was mosaic.

Conclusions Upd(14)mat and epimutation of 14q32.2 represent clinically discernible phenotypes and should be designated "upd(14)mat syndrome." This syndrome demonstrates a PWS-like phenotype particularly during infancy. The *MEG3* methylation test can detect upd(14)mat syndrome defects and should therefore be performed for all undiagnosed infants with hypotonia. *(J Pediatr 2009;155:900-3)*.

Maternal uniparental disomy 14 (upd(14)mat) is characterized by prenatal and postnatal growth retardation, neonatal hypotonia, small hands and feet, feeding difficulty, and precocious puberty.[1] Chromosome 14q32.2 contains several imprinted genes, and loss of expression of paternally expressed genes including *DLK1* and *RTL1* is believed to be responsible for upd(14)mat phenotype.[2] Thus far, 5 patients with epimutations and 4 patients with a microdeletion affecting the 14q32.2 imprinted region have been reported to have upd(14)mat-like phenotype.[2-4] Paternal uniparental disomy 14 (upd(14)pat) shows a distinct and much more severe phenotype characterized by facial abnormality, bell-shaped thorax and abdominal wall defects.[1] Initially, upd(14)mat was identified in patients with Robertsonian translocations involving chromosome 14, but increasing numbers of patients with a normal karyotype have been recognized.[1,5] Because maternal uniparental disomy 15 is responsible for the condition in more than 20% of patients with Prader-Willi syndrome (PWS), of which the overall prevalence is more than 1 in 15000 births,[6] one could suspect that upd(14)mat is underestimated. Phenotype of upd(14)mat is known to resemble that of PWS, which is characterized by neonatal hypotonia, small hands and feet, mental retardation, and hyperphagia resulting in obesity beyond infancy. Mitter et al[7] recently reported that upd(14)mat was detected in 4 of 33 patients who were suspected to have PWS and raised the question that upd(14)mat could be present in patients with PWS-like phenotype. Thus we examined patients who presented with PWS-like phenotype, but in whom PWS had been excluded.

Methods

The median age of the 78 patients enrolled in the study was 18.5 months, and the range was 1.4 to 324 months. Sex ratio was 1:1. All patients demonstrated PWS-like phenotype including hypotonia during infancy. We initially performed the *SNURF-SNRPN* DNA methylation test, and normal methylation results excluded the diagnosis of PWS.[8]

This study was approved by the Institutional Review Board Committees at Hokkaido University Graduate School of Medicine and National Center for Child Health and Development. The parents of the patients gave written informed consent.

DNA methylation status at the promoter region of imprinted *MEG3,* located in 14q32.2, was examined (Figure 1). Genomic DNA was extracted from leukocytes and treated with sodium bisulfite, and methylated allele– and unmethylated allele–specific primers were used to polymerase chain reaction amplify each allele, as described previously.[9] If aberrant DNA methylation was identified,

PWS	Prader-Willi syndrome
Upd(14)mat	Maternal uniparental disomy 14
Upd(14)pat	Paternal uniparental disomy 14

From the Department of Pediatrics, Hokkaido University Graduate School of Medicine, Sapporo (K.H., S.S.), the Department of Endocrinology and Metabolism (M.Kagami, T.O.), the Division of Clinical Genetics and Molecular Medicine (T.T.), and the Department of Pediatric Neurology (M. Kubota), National Research Institute for Child Health and Development, Tokyo, the Division of Medical Genetics, Kanagawa Children's Medical Center, Yokohama (K.K.), the Department of Pediatrics, Yamagata University School of Medicine, Yamagata (M. Kato), the Department of Pediatrics, Obihiro Kosei Hospital, Obihiro (K.U.), and the Department of Pediatrics, Nishi-Niigata Chuo National Hospital, Niigata (J.T.), Japan

This work was partially supported by a grant from the Ministry of Education, Science and Culture of Japan. The authors declare no conflicts of interest.

0022-3476/$ - see front matter. Copyright © 2009 Mosby Inc. All rights reserved. 10.1016/j.jpeds.2009.06.045

we carried out microsatellite polymorphism analysis for 16 loci on chromosome 14 (ABI PRISM Linkage Mapping Set v2.5; Applied Biosystems, Foster City, California) with DNA from the patients and their parents (Figure 1). Polymerase chain reaction products were analyzed on an ABI310 automatic capillary genetic analyzer and with GeneMapper software (Applied Biosystems). If aberrant DNA methylation was identified but the patient demonstrated biparental origin of the chromosome 14s, we further examined the chromosomes for DNA methylation state, parental origin, and microdeletion in 14q32.2, as described previously.[2,3]

Results

We identified abnormal hypomethylation at the *MEG3* promoter in 5 of 78 patients (Figure 2). Almost complete lack of methylation was found in 4 patients (case 1 to 4), but 1 patient (case 5) demonstrated faint methylation. Polymorphism studies demonstrated that 3 (cases 2 to 4) of the 4 patients with complete lack of *MEG3* promoter methylation had complete upd(14)mat, but 1 patient (case 1) had inherited both parental alleles (Table I; available at www.jpeds.com). We further examined the DNA methylation state and microdeletion or segmental upd at 14q32.3, and concluded that this patient (case 1) had an epimutation. The detailed data have been reported previously.[3] The patient (case 5) with faint *MEG3* methylation was demonstrated to have 2 maternal alleles, as well as 1 paternal allele with lower signal intensity. This indicated mosaicism of upd(14)mat (80%) and a normal karyotype (20%) (Figure 3; available at www.jpeds.com).

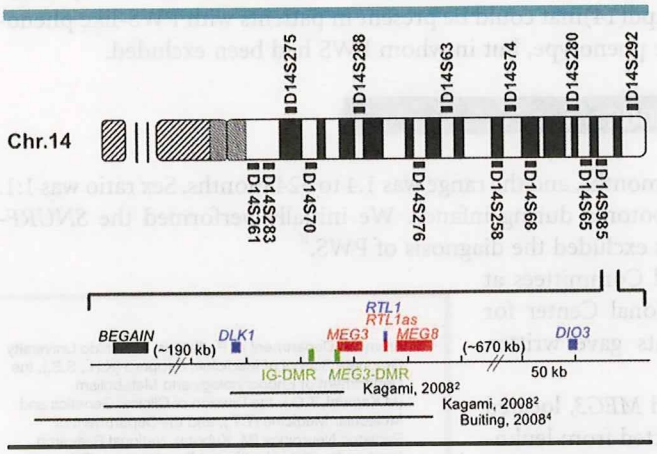

Figure 1. Schematic map of the 14q32.2 imprinted region. Loci on chromosome 14 represent markers used for microsatellite polymorphism analysis. Paternally expressed genes are shown in *blue*, maternally expressed genes in *red*, and nonimprinted genes are shown in *black*. Differentially methylated regions (DMRs) are shown in *green*. *IG-DMR,* Intergenic DMR. Reported microdeletions are demonstrated as *horizontal bars*.

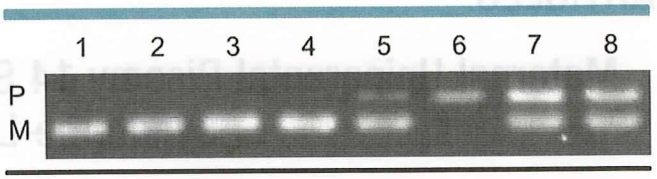

Figure 2. *MEG3* methylation test. *P,* Paternal methylated signal; *M,* maternal unmethylated signal; *1-5,* cases 1-5, respectively; *6,* paternal uniparental disomy 14; *7,* patient with PWS; *8,* normal control. Cases 1-4 show only the maternal unmethylated signal, and case 5 shows a faint paternal methylated signal.

The profiles of the patients with upd(14)mat or an epimutation are shown in Table II. We compared clinical features in these patients (Table III). All patients were referred to us during infancy because of hypotonia and motor developmental delay. Small hands and feet were also present in all patients. Prenatal growth retardation was present in all but 1 patient (case 1) who was later shown to have an epimutation. However, this patient had development of postnatal growth retardation, which was present in all patients. Premature onset of puberty was not evaluated in this study because the patients were too young. Apparent intellectual delay was only present in the patient who had upd(14)mat mosaicism (case 5). The clinical features of the patients with epimutation or with mosaic upd(14)mat were not distinct from those of the patients with full upd(14)mat.

Discussion

We detected 5 patients with upd(14)mat or epimutation at the 14q32.2-imprinted region in 78 subjects who had initially been suspected to have PWS. Mitter et al[7] reported that upd(14)mat was detected in 4 of 33 patients who were suspected to have PWS. However, Cox et al[10] reported that they did not find any upd(14)mat in 35 patients suspected to have PWS. Our study suggests that a significant number of patients with upd(14)mat are suspected to have PWS during infancy. To clarify how upd(14)mat and PWS share clinical features, we examined the clinical manifestations of our patients with upd(14)mat or an epimutation. All patients showed neonatal hypotonia and were referred to us during infancy. Feeding difficulty in the neonatal period and small hands and feet were also common to these patients and resembled features of PWS. It is noteworthy that all patients were referred during infancy, suggesting that upd(14)mat and PWS resemble each other, particularly during this period. Therefore upd(14)mat and related disorders, as well as PWS, should be important differential diagnoses for infants with hypotonia and feeding difficulty. Distinct features for upd(14)mat included less-specific facial characteristics, constant prenatal growth failure, and better intellectual development. Precocious puberty is not present in PWS; however, this was not evaluated in this study because the patients were not

Table II. Profiles of the patients with upd(14)mat and epimutation of 14q32.2

	Case 1	Case 2	Case 3	Case 4	Case 5
Molecular class	Epimutation	Upd(14)mat	Upd(14)mat	Upd(14)mat	Upd(14)mat (mosaic)
Age	2 y 2 m	4 y 2 m	2 y 7 m	1 y 9 m	3 y 4 m
Sex	Female	Male	Female	Female	Female
Karyotype	46,XX	46,XY	46,XX	46,XX	46,XX
Gestational age	41 w 5d	36 w 1 d	37 w 3 d	40 w 4 d	36 w
Birth weight g (SD)	3034 (0)	1955 (−2.6)	1680 (−3.3)	1858 (−2.8)	1434 (−3.9)
Birth length cm (SD)	50 (+0.7)	45.7 (−1.5)	40 (−4.0)	45 (−1.6)	39 (−3.9)
Birth OFC cm (SD)	Unknown	32 (−1.0)	30.4 (−2.0)	32 (−0.8)	30 (−2.2)
Present height cm (SD)	76.1 (−3.1)	89.5 (−2.8)	79 (−2.7)	72.5 (−3.4)	77.8 (−4.5)
Present weight kg (SD)	8.18 (−2.4)	11.6 (−2.1)	8.4 (−2.8)	6.4 (−3.7)	8.84 (−3.3)
Present OFC cm (SD)	45.2 (−1.5)	51.0 (+0.5)	48 (0)	44 (−1.8)	46.0 (−1.6)

old enough to demonstrate this feature. It is possible that when the patients get older, the clinical features of upd(14)mat may become more distinct from those of PWS.

We detected an epimutation in the 14q32.2-imprinted region, as well as upd(14)mat. The clinical features of the patient with the epimutation were grossly similar to those of patients with upd(14)mat. Thus far 5 patients with an epimutation in the paternal allele, including our patient, have been identified.[4,11] These patients exhibit clinical features indistinguishable from those with full upd(14)mat. Our patient with an epimutation demonstrated normal birth weight, but previously reported patients with an epimutation have shown intrauterine growth retardation. [4,11] Therefore normal birth weight is not a specific feature related to epimutation.

One of the patients with upd(14)mat was mosaic for upd(14)mat and normal karyotype. It is not easy to understand the pathogenesis of such a mosaic, but similar mosaicism of chromosome 15 has been reported.[12] Mosaicism for upd(15)mat and normal cell lines has been found in a patient with the PWS phenotype.[12] Similarly, our patient with mosaic upd(14)mat demonstrated typical clinical features of upd(14)mat. This could be explained by the small proportion of normal cell lines (less than 20%), or it could be that the level of mosaicism is different in each tissue. It is possible that the proportion of normal cells may be lower in the brain, which is most responsible for the phenotype of upd(14)mat.

As is clear in our series of patients, upd(14)mat phenotype can be caused by an epimutation of 14q32.2. Recently, Kagami et al[2] reported a microdeletion in 14q32.2 associated with a similar phenotype (Figure 1). Buiting et al[4] also reported a patient with a 1Mb deletion at 14q32.2 (Figure 1). Therefore upd(14)mat phenotype is associated with not only upd(14)mat but an epimutation or small deletion. This genetic complexity is similar to that of PWS. PWS is caused by paternal deletion of 15q11-q13, maternal uniparental disomy of chromosome 15, and epimutation (imprinting defect). A new name such as upd(14)mat syndrome would be appropriate to represent the entire upd(14)mat clinical features represented by upd(14)mat, epimutation of 14q32.2 and microdeletion in 14q32.2. Alternatively, Buiting et al[4] suggested the term, "Temple syndrome," because upd(14)mat was first described by Dr. I. K. Temple in 1991, who subsequently described an epimutation in 2007.[4,5,11]

Finally, it should be emphasized that the *MEG3* methylation test could detect not only upd(14)mat but an epimutation and small deletions involving *MEG3*.This is because the *MEG3* DMR that is used for the diagnostic DNA methylation test is involved in the shortest region of overlap of the microdeletions (Figure 1). It is therefore a powerful method for screening patients with upd(14)mat syndrome.

Table III. Clinical features in patients with upd(14)mat, epimutation and microdeletions of 14q32.2

	Present study					Previous studies		
	Case 1	Case 2	Case 3	Case 4	Case 5	Upd(14)mat (n = 35)	Epimutation (n = 4)	Microdeletion (n = 4)
Premature delivery	−	−	−	−	−	10/25	0/4	0/3
Prenatal growth failure	−	+	+	+	+	24/27	4/4	3/3
Postnatal growth failure	+	+	+	+	+	26/32	3/4	3/3
Somatic features	+	+	+	+	+	23/35	4/4	3/3
Frontal bossing	+	+	+	+	−	9/9		
High arched palate	−	+	+		+	7/9		
Micrognathia	+	+	−	+	+	5/5		
Small hands	+	+	+	+	+	24/27	4/4	3/3
Scoliosis	−	−	−	−	−	5/19		
Others								
Hypotonia	+	+	+	+	+	25/28	4/4	1/1
Obesity	−	−	−	−	−	14/34	3/4	1/4
Early onset of puberty	NA	NA	NA	NA	NA	14/16	3/4	2/3
Mental retardation	−	−	−	−	+	10/27	2/4	1/4

NA, Not applicable.
Previous studies are based on references 2, 3 and 4.

Upd(14)mat syndrome demonstrates PWS-like phenotype during infancy, and it should be considered when seeing a patient with hypotonia. The *MEG3* methylation test should be performed to identify this syndrome. ■

The authors thank Dr. T. Ariga for critical reading of the manuscript.

Submitted for publication Mar 20, 2009; last revision received May 6, 2009; accepted Jun 22, 2009.

Reprint requests: Shinji Saitoh, MD, PhD, Department of Pediatrics, Hokkaido University, Graduate School of Medicine, North 15, West 7, Kita-ku, Sapporo, 060-8638, Japan. E-mail: ss11@med.hokudai.ac.jp.

References

1. Kotzot D, Utermann G. Uniparental disomy (UPD) other than 15: phenotypes and bibliography updated. Am J Med Genet A 2005;136:287-305.
2. Kagami M, Sekita Y, Nishimura G, Irie M, Kato F, Okada M, et al. Deletions and epimutations affecting the human 14q32.2 imprinted region in individuals with paternal and maternal upd(14)-like phenotypes. Nat Genet 2008;40:237-42.
3. Hosoki K, Ogata T, Kagami M, Tanaka T, Saitoh S. Epimutation (hypomethylation) affecting the chromosome 14q32.2 imprinted region in a girl with upd(14)mat-like phenotype. Eur J Hum Genet 2008;16:1019-23.
4. Buiting K, Kanber D, Martín-Subero JI, Lieb W, Terhal P, Albrecht B, et al. Clinical features of maternal uniparental disomy 14 in patients with an epimutation and a deletion of the imprinted DLK1/GTL2 gene cluster. Hum Mutat 2008;29:1141-6.
5. Temple IK, Cockwell A, Hassold T, Pettay D, Jacobs P. Maternal uniparental disomy for chromosome 14. J Med Genet 1991;28:511-4.
6. Nicholls RD, Saitoh S, Horsthemke B. Imprinting in Prader-Willi and Angelman syndromes. Trends Genet 1998;14:194-200.
7. Mitter D, Buiting K, von Eggeling F, Kuechler A, Liehr T, Mau-Holzmann UA, et al. Is there a higher incidence of maternal uniparental disomy 14 [upd(14)mat]? Detection of 10 new patients by methylation-specific PCR. Am J Med Genet A 2006;140:2039-49.
8. Kubota T, Das S, Christian SL, Baylin SB, Herman JG, Ledbetter DH. Methylation-specific PCR simplifies imprinting analysis. Nat Genet 1997;16:16-7.
9. Murphy SK, Wylie AA, Coveler KJ, Cotter PD, Papenhausen PR, Sutton VR, et al. Epigenetic detection of human chromosome 14 uniparental disomy. Hum Mutat 2003;22:92-7.
10. Cox H, Bullman H, Temple IK. Maternal UPD(14) in the patient with a normal karyotype: clinical report and a systematic search for cases in samples sent for testing for Prader-Willi syndrome. Am J Med Genet A 2004;127A:21-5.
11. Temple IK, Shrubb V, Lever M, Bullman H, Mackay DJ. Isolated imprinting mutation of the DLK1/GTL2 locus associated with a clinical presentation of maternal uniparental disomy of chromosome 14. J Med Genet 2007;44:637-40.
12. Horsthemke B, Nazlican H, Hüsing J, Klein-Hitpass L, Claussen U, Michel S, et al. Somatic mosaicism for maternal uniparental disomy 15 in a girl with Prader-Willi syndrome: confirmation by cell cloning and identification of candidate downstream genes. Hum Mol Genet 2003;12:2723-32.

Table I. Microsatellite polymorphism analyses for chromosome 14 in 6 families with aberrant MEG3 methylation

Locus	Region	Case 1 family			Case 2 family			Case 3 family			Case 4 family			Case 5 family		
		Patient	Father	Mother	Patient	Father	Mother	Patient	Father	Mother	Patient	Father	Mother	Patient	Father	Mother
D14S261	14q11.2	298, 298	274, 298	298, 298	297, 297	297, 299	297, 297	298, 298	296, 298	298, 298	297, 297	297, 297	275, 297	275, 297, 297	275, 299	273, 297
D14S283	14q11.2	147, 149	139, 149	137, 147	139, 139	137, 137	139, 139	137, 149	133, 137	137, 149	150, 150	142, 150	140, 150	139, 139	137, 139	139, 147
D14S275	14q12	146, 146	146, 156	146, 146	149, 149	145, 145	149, 151	148, 152	146, 146	148, 152	155, 155	149, 155	149, 155	146, 148, 152	152, 156	146, 148
D14S70	14q13.1	100, 102	102, 102	100, 104	101, 101	101, 103	101, 101	103, 103	99, 101	103, 103	104, 104	104, 106	104, 104	101, 101, 103	101, 103	101, 101
D14S288	14q21.2	191, 201	201, 203	191, 207	201, 201	203, 203	201, 201	193, 193	193, 203	193, 193	195, 195	213, 215	195, 197	190, 196, 204	188, 196	190, 204
D14S276	14q22.3	241, —	239, 241	247, —	242, 244	244, 246	242, 244	244, 244	242, 244	244, 244	245, 245	241, 241	245, 245	244, 246, 246	242, 244	246, 246
D14S63	14q23.2	187, 187	187, 187	187, 187	187, 193	183, 189	187, 193	183, 187	189, 191	183, 187	191, 191	185, 195	191, 195	187, 189, 193	187, 193	187, 189
D14S258	14q24.2	204, 206	196, 206	202, 204	196, 196	198, 202	196, 196	196, 196	200, 202	196, 196	202, 202	204, 204	202, 204	196, 196, 198	198, 200	196, 196
D14S74	14q24.3	299, 313	260, 299	303, 313	303, 303	303, 305	303, 303	299, 303	299, 301	299, 303	295, 295	305, 313	295, 301	299, 301, 305	299, 305	299, 301
D14S68	14q31.3	323, 323	323, 323	323, 323	321, 321	323, 323	321, 321	321, 323	323, 323	321, 323	323, 323	325, 325	321, 323	321, 321, 323	323, 323	321, 321
D14S280	14q32.12	246, 248	248, 248	246, 246	243, 243	243, 245	243, 243	247, 247	243, 247	247, 247	248, 248	244, 244	242, 248	241, 243, 247	241, 245	243, 247
D14S65	14q32.2	135, 141	135, 135	135, 141	145, 145	135, 149	135, 145	135, 147	137, 145	135, 147	150, 150	150, 150	150, 150	135, 147	147, 147	135, 147
D14S985	14q32.2	255, 255	251, 255	255, 257	250, 250	246, 254	250, 254	247, 247	249, 249	247, 247	248, 248	246, 248	248, 254	247, 249	247, 253	247, 249
D14S292	14q32.33	84, 86	84, 86	86, 86	92, 92	86, 88	88, 92	85, 87	83, 85	85, 87	92, 92	86, 92	88, 92	87, 89	89, 89	87, 89

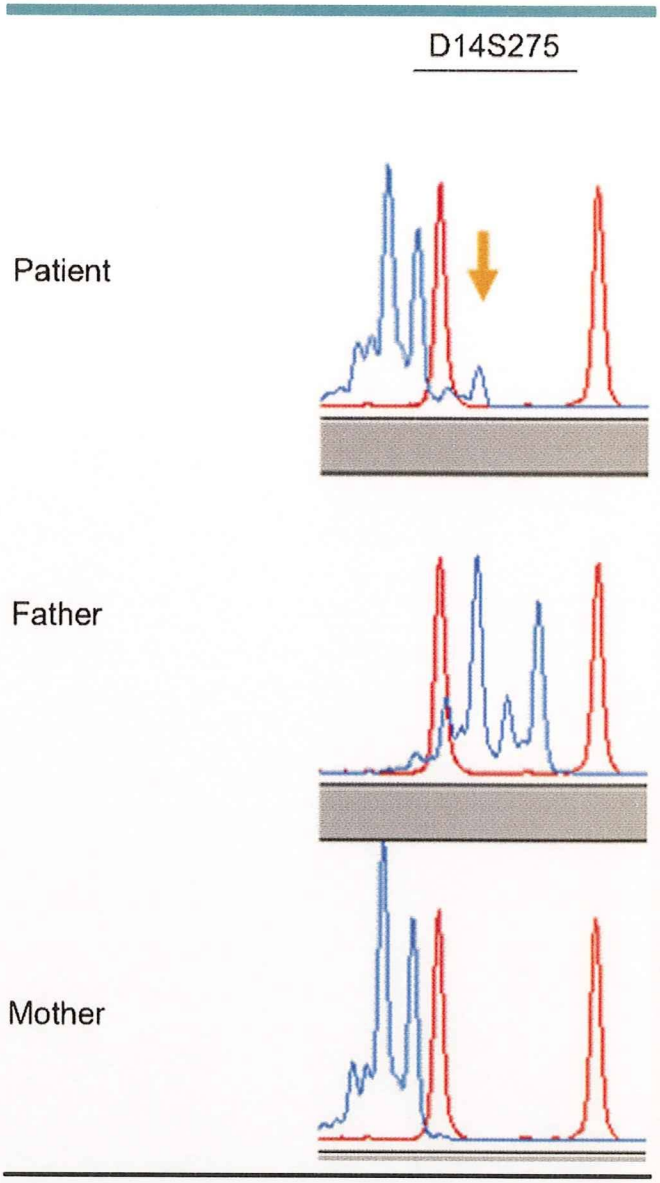

Figure 3. Microsatellite polymorphism analysis at D14S275 for the family of case 5. The patient demonstrates 3 peaks (146, 148, 152 bp), 2 (146, 148 bp) of which are transmitted from the mother, but 1 small peak (152 bp) indicated by the *arrow* is transmitted from the father. *Red peaks* depict size markers.

Neuroradiology (2009) 51:821–830
DOI 10.1007/s00234-009-0579-7

DIAGNOSTIC NEURORADIOLOGY

Clinical and imaging characteristics of localized megalencephaly: a retrospective comparison of diffuse hemimegalencephaly and multilobar cortical dysplasia

Masumi Nakahashi · Noriko Sato · Akira Yagishita · Miho Ota · Yoshiaki Saito · Kenji Sugai · Masayuki Sasaki · Jun Natsume · Yoshito Tsushima · Makoto Amanuma · Keigo Endo

Received: 15 May 2009 / Accepted: 22 July 2009 / Published online: 12 August 2009
© Springer-Verlag 2009

Abstract
Introduction Hemimegalencephaly is a well-known congenital malformation. However, localized megalencephaly, which may be one of the subtypes of hemimegalencephaly, has not been separately investigated. In the present study, we attempted to characterize the clinical and magnetic resonance (MR) imaging features of localized megalencephaly in comparison with ordinary diffuse hemimegalencephaly and multilobar cortical dysplasia.
Methods MR findings for 43 patients with hemimegalencephaly and ten with multilobar cortical dysplasia, which is the differential diagnosis of localized megalencephaly, were retrospectively reviewed. Clinical findings such as the onset and severity of seizures and imaging findings including the affected area of the brain, structures outside of the hemisphere, and interval morphological changes were examined.
Results Of the 43 patients, 11 showed signs of localized megalencephaly (25.6%). Localized megalencephaly was predominantly seen on the left side (72.7%) and had a tendency toward severe-grade seizures compared to multilobar cortical dysplasia. The frequencies of the extracerebral abnormalities in the diffuse hemimegalencephaly, localized megalencephaly, and multilobar cortical dysplasia groups were 84.4%, 36.4%, and 0.0%, respectively. There were three localized megalencephaly patients whose affected areas shrank and whose images were similar to those of multilobar cortical dysplasia.
Conclusion Localized megalencephaly accounts for one quarter of all hemimegalencephaly cases in this study. The incidence of extracerebral abnormalities in patients with localized hemimegalencephaly was almost half that of patients with diffuse hemimegalencephaly. Extracerebral abnormalities were absent in patients with multilobar cortical dysplasia. Associated extracerebral abnormalities may be a clue to differentiating localized megalencephaly from multilobar cortical dysplasia.

Keywords Hemimegalencephaly · Localized megalencephaly · Multilobar cortical dysplasia · Extracerebral abnormality

M. Nakahashi · Y. Tsushima · M. Amanuma · K. Endo
Department of Diagnostic Radiology and Nuclear Medicine,
Gunma University Graduate School of Medicine,
Maebashi, Gunma, Japan

N. Sato (✉) · M. Ota
Department of Radiology,
National Center Hospital of Neurology and Psychiatry,
4-1-1 Ogawahigashi-chyo,
Kodaira, Tokyo 187-8551, Japan
e-mail: snoriko@ncnp.go.jp

Y. Saito · K. Sugai · M. Sasaki
Department of Child Neurology,
National Center Hospital of Neurology and Psychiatry,
Kodaira, Tokyo, Japan

A. Yagishita
Department of Neuroradiology,
Tokyo Metropolitan Neurological Hospital,
Kokubunji, Tokyo, Japan

J. Natsume
Department of Pediatrics,
Nagoya University Graduate School of Medicine,
Nagoya, Aichi, Japan

Introduction

Hemimegalencephaly (also termed unilateral megalencephaly) is a relatively rare but clinically impressive brain malformation

characterized by unilateral hemispheric enlargement, cytoarchitectural abnormalities, and an association with epilepsy [1–8]. Despite the multitude of antiepileptic drugs available, the treatment of epilepsy associated with malformations of cortical development may require cortical resection or hemispherotomy/hemispherectomy [9]. The pathogenesis of malformations of cortical development such as focal cortical dysplasia, hemimegalencephaly, or polymicrogyria, remains unknown [10]. However, the etiology of hemimegalencephaly is presumed to be abnormalities of neuroglial differentiation and cell migration involving a single hemisphere [11–16]. It has recently been reported that various morphological abnormalities occurring outside the involved hemisphere, such as ipsilateral olfactory nerve enlargement, cerebral vascular dilatations, cerebellar enlargement, and abnormal architecture of the bilateral or ipsilateral cerebellar folia, are often associated with hemimegalencephaly [17].

In hemimegalencephaly, the extensive dysplasia usually involves an entire cerebral hemisphere but sometimes only appears over a partial area of one hemisphere. Such cases are variously called "localized megalencephaly" [18], "hemi-hemimegalencephaly" [19], or "focal megalencephaly" [20]. To the best of our knowledge, there has been only one original manuscript related to localized megalencephaly; that report characterized the clinical features of 19 patients with posterior quadrantic dysplasia, including both localized megalencephaly (hemi-hemimegalencephaly) and focal cortical dysplasia, and evaluated postoperative outcomes in these patients [19]. There have also been several original studies of hemimegalencephaly that included patients with localized megalencephaly without actually focusing on it [20–23]. Therefore, localized megalencephaly is not commonly recognized.

Focal cortical dysplasia is an important differential diagnosis of localized megalencephaly. Focal cortical dysplasia usually appears as a focal area of abnormal cortical thickness and poor gray/white matter differentiation. It is usually limited to a focal area of the brain but can sometimes involve multiple gyri, occupying one or more lobes. This condition is known as multilobar cortical dysplasia [19]. In hemimegalencephaly, the affected area of the enlarged cerebral hemisphere might occasionally become atrophic if seizures are not well controlled [24]. In such cases, it is difficult to distinguish localized megalencephaly from multilobar cortical dysplasia. These atypical postatrophic magnetic resonance (MR) findings of localized megalencephaly have not been well recognized. Therefore, in addition to the poor recognition of localized megalencephaly, it is even more difficult to diagnose atypical localized megalencephaly.

In this study, to characterize MR findings of localized megalencephaly, we retrospectively reviewed 43 patients with hemimegalencephaly, which represents the largest number of such cases studied to date, and investigated the clinical and MR imaging findings in patients with localized megalencephaly and ordinary diffuse hemimegalencephaly. At the same time, multilobar cortical dysplasia, which is the differential diagnosis of localized megalencephaly, was also examined.

Methods

Patients

We retrospectively reviewed radiological reports of patients with a diagnosis of hemimegalencephaly in two neurological specialty hospitals and of cortical dysplasia in one hospital from January 1998 to January 2009. All of the patients were admitted for intractable epilepsy and underwent detailed examinations to determine whether surgical treatment was indicated. There were 43 hemimegalencephaly and 65 cortical dysplasia patients according to radiological reports. We defined hemimegalencephaly as the enlargement of all or part of one hemisphere [18–22]. Constant features were gross asymmetry with enlargement

Table 1 Clinical features of ordinary diffuse hemimegalencephaly, localized megalencephaly, and multilobar cortical dysplasia.

	No. of patients	Mean age (range, median age)	Sex (male: female)	Mean age of seizure onset (range, median age)	Epilepsy grade before operation[a]		
					Grade 1	Grade 2	Grade 3
Diffuse hemimegalencephaly	32	2.7±5.4 years (1 month–25 years, 6 months)	19:13	40.0±66.7 days (0–240, 7.0 days)	4	21	7
Localized megalencephaly	11	2.8±5.6 years (2 months–19 years, 8 months)	6:5	20.7±29.8 days (0–90, 3.0 days)	2	7	2
Multilobar cortical dysplasia	10	3.7±6.2 years (3 months–21 years, 1.5 years)	5:5	187.2±210.4 days (7–660, 75.0 days)	1	9	0

[a] Grade 1: mild = well-controlled by medication; 2: moderate = not well-controlled by medication, but with a seizure incidence of less than 100 a day; 3: severe = uncontrolled by medication with more than 100 seizures per day

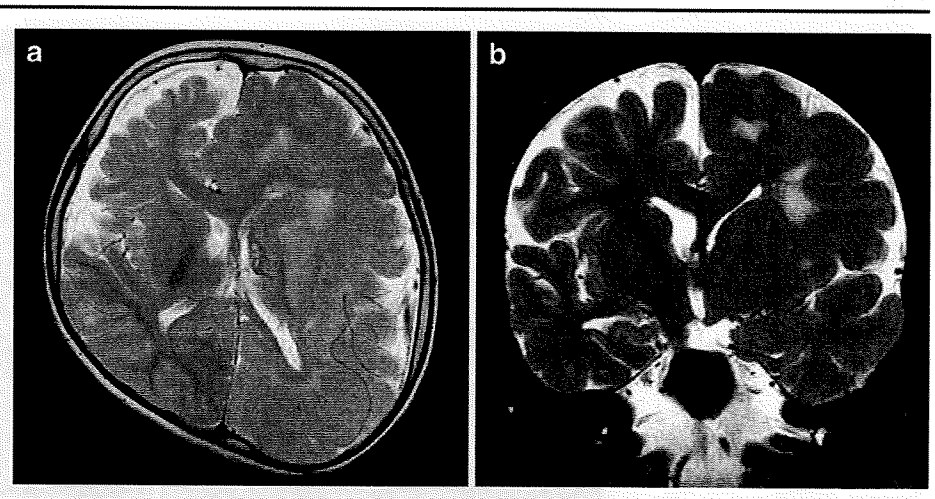

Fig. 1 MR images of left hemimegalencephaly in an 8-year-old boy with grade 2 seizures and status epilepticus from the age of 2 days. **a**, **b** Axial and coronal T2-weighted images show his affected enlarged displastic area extending to the entire left hemisphere. This type is classified as ordinary diffuse hemimegalencephaly

of one hemisphere, dysplastic cortex, and asymmetry and deformity of the ventricular system [8]. In addition to diffuse or focal unilateral cerebral enlargement, other radiological findings such as cortical thickening, broad gyri, shallow sulci, enlargement of the ipsilateral lateral ventricle, straightening of the ipsilateral frontal horn, heterogeneity of the white matter, poor cortical-white matter differentiation, and abnormally advanced myelination were considered in making the diagnosis [18]. We defined diffuse hemimegalencephaly as the enlargement of the entire hemisphere. If the affected enlarged region of the brain was localized, we defined it as localized megalencephaly. Furthermore, in the localized megalencephaly group, the regions of the affected lobes were roughly grouped into three types: the frontal-lobe-dominant type (anterior quadrantic type), the occipital-lobe-dominant type (posterior quadrantic type) [19], and the almost-diffuse type. In the almost-diffuse type, the affected area was over three lobes but not the entire ipsilateral hemisphere. Hemimegalencephaly was diagnosed using imaging findings such as MR with reference to clinical and other radiological examinations and was not established on the basis of pathology. MR images of the 43 patients with hemimegalencephaly were reviewed by three neuroradiologists (M.N., N.S., and H.O., with 7, 20, and 22 years of experience with MR imaging, respectively). The results were determined by consensus of the three readers. All serial images obtained for each patient were reviewed at the same time. All 43 patients were diagnosed with hemimegalencephaly; there were 32 diffuse-type cases (19 males, 13 females; mean age 2.7± 5.4 years; range 1 month–25 years) and 11 localized-type cases (six males, five females; mean age 2.8±5.6 years; range 2 months–19 years). Twenty patients with diffuse hemimegalencephaly and seven patients with localized megalencephaly underwent an operation. Twelve patients with diffuse hemimegalencephaly and four patients with localized megalencephaly were treated by means of medication.

On the other hand, the patients with cortical dysplasia were selected by pathological confirmation. Out of the 65 suspected cortical dysplasia cases based on radiological reports, 26 patients underwent operations. Twenty-five of

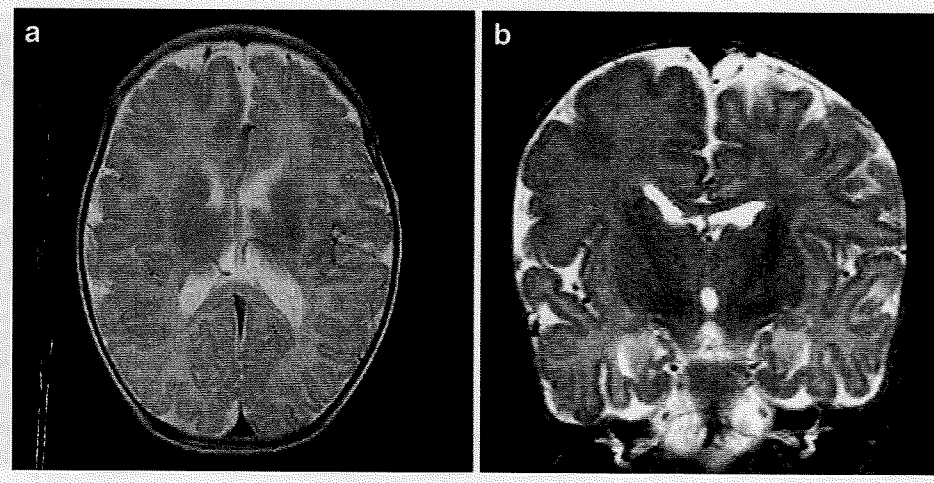

Fig. 2 MR images from a 2-month-old girl with right localized megalencephaly in whom seizures commenced at 2 days of age and continued at a frequency of approximately 12 per day (grade 2). **a**, **b** Axial and coronal T2-weighted images show a focally enlarged frontal lobe in patients with localized hemimegalencephaly in the right hemisphere (frontal-lobe-dominant type)

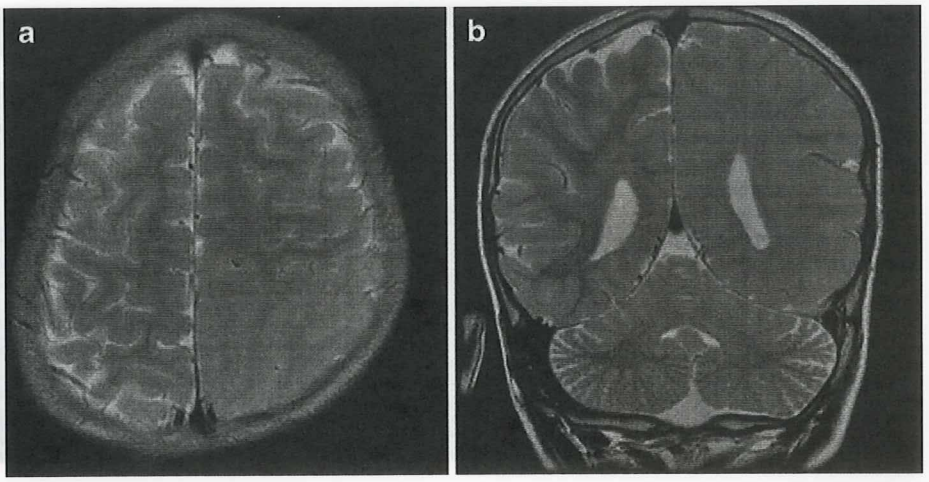

Fig. 3 MR images of left localized megalencephaly in a 6-year-old boy with very severe grade 3 seizures and status epilepticus from the age of 3 days. **a**, **b** Axial and coronal T2-weighted images show focally enlarged occipital and parietal lobes with ill-defined gray and white matter differentiation (occipital-lobe-dominant type)

them were pathologically diagnosed as having cortical dysplasia, and it was concluded that one patient showed no significant alterations. Three neuroradiologists, as mentioned above, evaluated the MR imagings to differentiate multilobar cortical dysplasia from usual focal cortical dysplasia. Multilobar cortical dysplasia was considered to exist when the affected region extended over multiple gyri or when it occupied several lobes [19]. Fifteen patients had focal cortical dysplasia, and ten patients had multilobar cortical dysplasia (five males, five females; mean age 3.7±6.2 years; range 3 months–21 years). This study had appropriate Ethics Committee approval.

MR imaging

MR scans were performed on 1-T or 1.5-T imagers. Sequences included T1-weighted images (TR/TE, 300–624/9–15 ms; field of view [FOV], 220×220 or 220×165; section thickness, 4–7/0.5–1.7-mm gap; matrix, 256×224, 256×256, or 512×448; NEX, 2 or 3), T2-weighted images (TR/TE, 4,000–4,200/95–121 ms; FOV, 220×220 or 220×165; section thickness, 3–6/0.5–1.7-mm gap; matrix, 256×224, 256×256, or 512×432; NEX, 1), fluid-attenuated inversion recovery images (TR/TE/TI, 8,000–10,002/104–158/2,200–2,500 ms; FOV, 220×220; section thickness, 5–6/1–2.5-mm gap; matrix, 256×192, 256×256, or 512×432; NEX, 1), inversion recovery images (TR/TE/TI, 4,000–4,210/32–85/120–150 ms; FOV, 220×220, 220×165; section thickness, 3–4/0.3–2-mm gap; matrix, 256×256 or 512×432; NEX, 2 or 3), and 3D high-resolution sagittal T1-weighted fast, low-angle shot gradient echo images (TR/TE/TI, 1,970/3.9/110 ms; flip angle, 15°; FOV, 315×315; effective section thickness, 1.2 mm; slab thickness, 177 mm; 3D partitions, 144 slices; matrix, 512×228; NEX, 1). Three different planes were obtained in all MR examinations except in three studies, which included the axial and coronal planes. Each examination included four to nine sequences. In all cases, MR examinations were performed in the whole brain, and we evaluated which areas of the cerebrum were affected as well as extracerebral

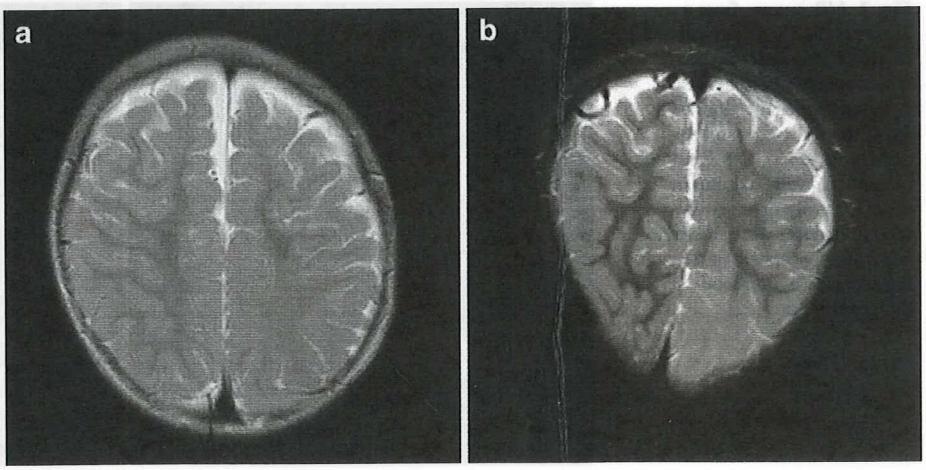

Fig. 4 MR images from a 2-year-old girl with left multilobar cortical dysplasia. Seizure onset was at 2 months of age, and seizure frequency was one to two per day (grade 2). **a**, **b** Axial and coronal T2-weighted images indicate poor differentiation of gray and white matter in the left parietal lobe without enlargement

Table 2 Imaging features of ordinary diffuse hemimegalencephaly, localized megalencephaly, and multilobar cortical dysplasia.

	No. of patients	Affected cerebral hemisphere (right:left)	Extent of affected lobe	No. of patients	Extracerebral abnormalities (%)
Diffuse hemimegalencephaly	32	19:13			27/32 (84.4)
Localized megalencephaly	11	3:8	Almost-diffuse type (except for the inferior temporal and inferior parietal lobes)	2	4/11 (36.4)
			Frontal-lobe-dominant type (frontal and temporal lobes dominant)	4	
			Occipital-lobe-dominant type (occipital and parietal lobes dominant)	5	
Multilobar cortical dysplasia	10	3:7	Frontal lobe	4	0/10 (0.0)
			Occipital and parietal lobes	3	
			Temporal lobe	3	

findings. Thirty-one patients with hemimegalencephaly and six patients with multilobar cortical dysplasia each underwent one preoperative MR examination. Twelve patients with hemimegalencephaly (interval 1–62 months) and four patients with multilobar cortical dysplasia (interval 1–11 months) underwent preoperative MR examinations more than twice.

Clinical and imaging characteristic interpretation

Clinical and imaging findings were evaluated in the three groups: diffuse hemimegalencephaly, localized megalencephaly, and multilobar cortical dysplasia. Clinical evaluations included age, sex, mean age of seizure onset, and severity of seizures. Data were expressed as the mean± standard deviation. Since there is no appropriate classification of the severity of seizures apart from Engel's classification, which is used to judge the efficacy of surgery, we originally classified seizure severity into three grades: grade 1, well-controlled by medication; grade 2, not well-controlled by medication, but with a seizure incidence of less than 100 a day; and grade 3, uncontrolled by medication with more than 100 seizures per day. MR imaging findings were also used to evaluate the affected cerebral side and structures outside of the hemisphere, including ipsilateral cranial nerve enlargement (only large cranial nerves such as the olfactory, optic, and trigeminal nerves being evaluated), dilatation of cerebral vasculature, brainstem and cerebellar asymmetry, and abnormal cerebellar folias. In the localized megalencephaly and multilobar cortical dysplasia groups, the affected cerebral areas were also evaluated. In the localized megalencephaly group, the regions of the affected lobes were roughly grouped into three types as described above. Furthermore, in patients who received preoperative MR examinations more than twice, serial parenchymal morphologic changes of the affected areas such as atrophy were also assessed. All MR images were evaluated by three neuroradiologists, as mentioned above. The results were determined by consensus of the three readers. All serial images obtained for each patient were reviewed at the same time.

Results

Table 1 summarizes the clinical characteristics of diffuse and localized megalencephaly and of multilobar cortical dysplasia. Of the 43 patients with hemimegalencephaly, 32

Table 3 Details of extracerebral abnormalities of ordinary diffuse hemimegalencephaly, localized megalencephaly, and multilobar cortical dysplasia.

	Olfactory nerve enlargement (%)	Optic nerve enlargement (%)	Vascular dilatations (%)	Cerebellar asymmetry (%)	Abnormal folia		Brain stem asymmetry (%)
					In ipsilateral side (%)	In contralateral side (%)	
Diffuse hemimegalencephaly	10/32 (31.3)	1/32 (3.1)	10/32 (31.3)	18/32 (56.3)	7/32 (21.9)	3/32 (9.4)	3/32 (9.4)
Localized megalencephaly	2/11 (18.2)	0/11 (0.0)	3/11 (27.3)	1/11 (9.1)	2/11 (18.2)	0/11 (0.0)	0/11 (0.0)
Multilobar cortical dysplasia	0/10 (0.0)	0/10 (0.0)	0/10 (0.0)	0/10 (0.0)	0/10 (0.0)	0/10 (0.0)	0/10 (0.0)

patients (74.4%) exhibited the diffuse variety (Fig. 1), and 11 patients (25.6%) exhibited the localized variety (Figs. 2 and 3). The seizure onset of patients in the multilobar cortical dysplasia group (Fig. 4) was later than that in the hemimegalencephaly groups. Seizure severity was slightly milder in patients with multilobar cortical dysplasia.

Table 2 summarizes the imaging characteristics of the three groups. The left cerebral hemisphere was affected in about 70% of patients with localized megalencephaly and multilobar cortical dysplasia. The incidence was almost double that in patients with diffuse hemimegalencephaly (40.6%). In localized megalencephaly and multilobar cortical dysplasia, we could not define any significantly affected lobes.

Various extracerebral abnormalities were observed in diffuse hemimegalencephaly and localized megalencephaly (Tables 2 and 3). These findings were less frequently observed in the localized megalencephaly group than in patients with diffuse hemimegalencephaly. No patients with multilobar cortical dysplasia were observed.

Table 4 summarizes the clinical and imaging features of localized megalencephaly. Extracerebral abnormalities were least frequently observed in occipital-lobe-dominant type.

Furthermore, there were four hemimegalencephaly patients who had received more than two preoperative MR examinations whose affected area began to shrink. In atrophic cases, we obtained serial MR images and confirmed that they had shown the enlarged cerebral areas in the first examination before atrophy. One of these four patients had diffuse hemimegalencephaly and three had localized megalencephaly (Figs. 5 and 6). Three of the four had extracerebral abnormalities. On the other hand, no atrophic changes of the affected areas were noted during the follow-up in any patients with multilobar cortical dysplasia.

Twenty patients with diffuse hemimegalencephaly and seven patients with localized megalencephaly underwent an operation. They had variable histopathological findings such as polymicrogyria, cortical dysplasia, and gliotic tissue. There was no histopathological difference between diffuse hemimegalencephaly and localized megalencephaly. In addition, in two of the histologically confirmed cases of localized hemimegalencephaly, the focally enlarged areas had shrunk. There was no difference between the atrophic cases and nonatrophic cases.

Discussion

Our study characterized the clinical and imaging features of localized megalencephaly using whole-brain MR imaging. To the best of our knowledge, our study has the largest number of cases among hemimegalencephaly studies and is the first report focusing on clinical and imaging findings of localized

Table 4 Clinical and imaging features of localized megalencephaly.

	No. of patients	Mean age (range, median age)	Sex (male:female)	Mean age of seizure onset (range, median age)	Epilepsy grade before operation[a]			Affected cerebral hemisphere (right:left)	Extracerebral abnormalities (%)	Olfactory nerve enlargement (%)	Vascular dilatations (%)	Cerebellar asymmetry (%)	Abnormal folia in ipsilateral side (%)
					Grade 1	Grade 2	Grade 3						
Almost-diffuse type	2	3.0±1.4 months (2–4 months, 3 months)	1:1	29.0±21.2 days (14–44, 29.0 days)	0	2	0	1:1	1/2 (50.0)	0/2 (0.0)	1/2 (50.0)	0/2 (0.0)	0/2 (0.0)
Frontal-lobe-dominant type	4	6.3±4.6 months (2 months–1 year, 5.5 months)	1:3	15.0±27.3 days (0–56, 2.0 days)	1	3	0	1:3	2/4 (50.0)	2/4 (50.0)	1/4 (25.0)	1/4 (25.0)	1/4 (25.0)
Occipital-lobe-dominant type	5	67.6±93.5 months (5 months–19 years, 2.0 years)	4:1	22.0±38.4 days (1–90, 3.0 days)	1	2	2	1:4	1/5 (20.0)	0/5 (0.0)	1/5 (20.0)	0/5 (0.0)	1/5 (20.0)

[a] Grade 1: mild = well-controlled by medication; 2: moderate = not well-controlled by medication, but with a seizure incidence of less than 100 a day; 3: severe = uncontrolled by medication with more than 100 seizures per day

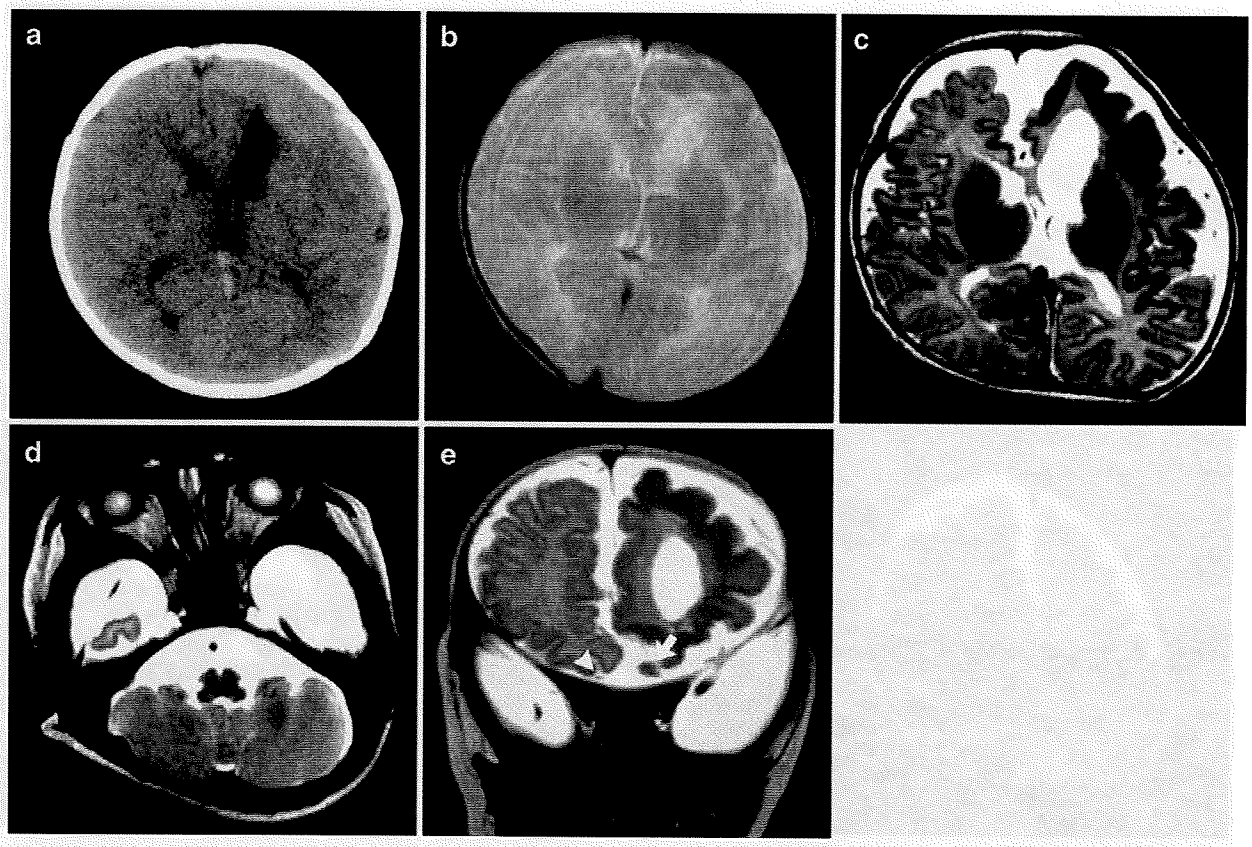

Fig. 5 Computer tomography (CT) and follow-up MR images of a boy with left localized megalencephaly in whom seizures commenced at 2 days of age and continued at a frequency of approximately ten per day (grade 2). **a**, **b** At 4 weeks of age, CT and axial T2-weighted images show focally enlarged frontal and temporal lobes in the left hemisphere (frontal-lobe-dominant type). **c** At 11 weeks of age, the axial T2-weighted image shows that his affected frontal area has turned atrophic. The left lateral ventricle is enlarged. The left intracalvarial volume is larger than the right. **d** Asymmetry of the hemicerebellum with abnormal folia is also observed in the left hemisphere. The left intracalvarial volume of the posterior fossa is larger than the right. **e** A coronal T2-weighted image also shows the affected left frontal lobe. The left olfactory nerve is asymmetrically enlarged (*arrow*) compared to the right (*arrowhead*). The left intracalvarial volume is enlarged in not only the frontal portion but also in the middle fossa

megalencephaly. We revealed that localized megalencephaly was not rare among cases of hemimegalencephaly, and indeed accounted for approximately one quarter of all hemimegalencephaly cases. Localized megalencephaly was predominantly seen on the left side and tended to induce more severe seizures than multilobar cortical dysplasia. The incidence of extracerebral abnormalities in patients with localized hemimegalencephaly was almost half that of patients with diffuse hemimegalencephaly. Extracerebral abnormalities were absent in patients with multilobar cortical dysplasia. Furthermore, extracerebral abnormalities were least frequently observed in occipital-lobe-dominant type. Findings of extracerebral abnormalities would therefore be useful in differentiating localized megalencephaly from multilobar cortical dysplasia.

In 1987, Kalifa et al. reported five patients with hemimegalencephaly. They studied computed tomography and MR images and compared the radiologic patterns of these patients to those of patients with other similar anomalies. In their study, two of five patients showed signs of localized megalencephaly (40.0%) [23]. In 1990, Barkovich et al. reported 12 patients with hemimegalencephaly and described the correlation between MR imaging and pathologic characteristics. Five of the 12 patients in their study had localized megalencephaly (41.2%) [22]. The incidence of the localized type was higher in their study than in ours, but their study included a much smaller number of patients than ours. In 2004, D'Agostino et al. reported 19 patients with posterior quadrantic dysplasia, including 14 cases of localized megalencephaly (hemi-hemimegalencephaly), without including diffuse hemimegalencephaly, and evaluated their postoperative outcomes. However, they did not mention the imaging characteristics of localized megalencephaly [19].

In terms of seizure severity, patients with multilobar cortical dysplasia showed milder seizures than patients with hemimegalencephaly in the present study. None of the

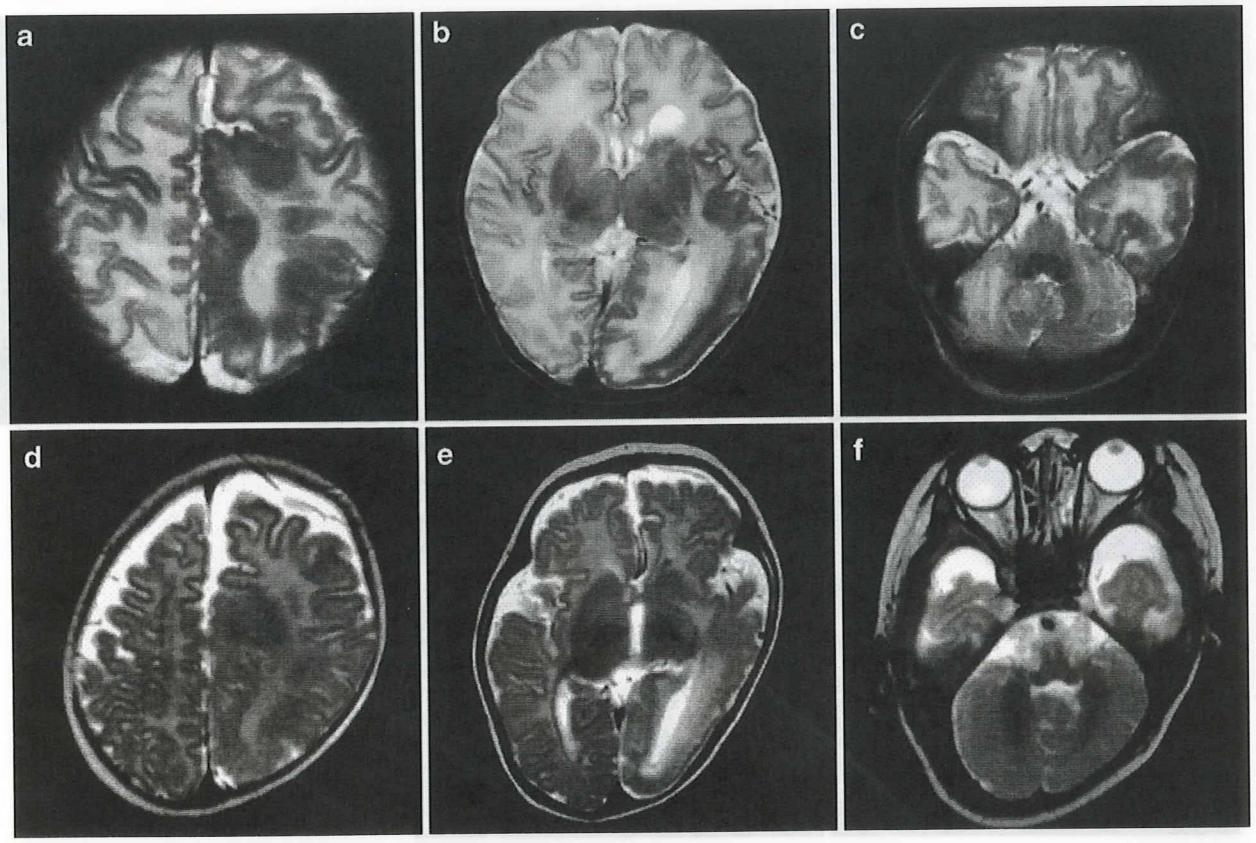

Fig. 6 Follow-up MR images of a boy with left localized megalencephaly in whom seizures commenced at 2 days of age and continued at a frequency of approximately ten to 20 per day (grade 2). **a**, **b** At 2 weeks of age, an axial T2-weighted image demonstrates that the parietal, posterior, and temporal lobes are enlarged in the left hemisphere (occipital-lobe-dominant type). **c** An axial T2-weighted image also shows abnormal folia of the hemicerebellum in the left hemisphere. **d**–**f** At 5 months of age, the axial T2-weighted MR images show atrophic left parietal and posterior lobes. Only the left parietal enlargement is preserved

patients with multilobar cortical dysplasia had grade 3 seizures, the most severe type, although the extent of the areas affected was not substantially different from that in localized megalencephaly. It is possible that fewer patients with multilobar cortical dysplasia became severely affected compared with those with diffuse or localized megalencephaly. D'Agostino et al. suggested that intractable epilepsy in posterior quadrantic dysplasia, including both localized megalencephaly (hemi-hemimegalencephaly) and multilobar cortical dysplasia, might be alleviated by a large quadrantic temporoparietooccipital resection instead of hemispherectomy, which is burdened by relatively high mortality and morbidity compared with more limited resections [19]. We therefore believe it is important to recognize localized megalencephaly and distinguish it from diffuse hemimegalencephaly in order to initiate therapy that would result in the most favorable outcome.

In localized megalencephaly and multilobar cortical dysplasia, the left cerebral hemisphere was found to be affected in about 70% of cases. This incidence was almost double that of patients with diffuse hemimegalencephaly. Kalifa et al. reported that the left cerebral hemisphere was affected in both their cases [23]. Barkovich et al. reported that, of their five localized megalencephaly patients, four were affected on the right side and one on the left side [22]. D'Agostino et al. reported that, of their 14 localized megalencephaly patients, four were affected on the right side and ten on the left side [19]. In those reports and our study, 21 of a total of 32 localized megalencephaly patients were affected on the left side (65.6%). The combined left-side-affected incidence for the two relatively large studies, that of D'Agostino et al. and ours, would be 72.0%. The reason the left side appears to be more frequently affected than the right is uncertain. However, the left hemisphere is the eloquent hemisphere and thus would lead to symptoms even when the lesions are small. The affected area of the right hemisphere may not be as noticeable in patients who had no symptoms. In localized megalencephaly, the regions

of the affected lobes were roughly grouped into three types: the frontal-lobe-dominant type (anterior quadrantic type), the occipital-lobe-dominant type (posterior quadrantic type), and the almost-diffuse type. In our study, the number of patients with the occipital-lobe-dominant type of megalencephaly was almost the same as that of those with the frontal-lobe-dominant type. Kalifa et al. reported that two of their cases were of the occipital-lobe-dominant type [23]. Barkovich et al. reported that, of their five hemimegalencephaly patients, one was of the frontal-lobe-dominant type, two were of the occipital-lobe-dominant type, and two were of the almost-diffuse type [22].

There were 12 hemimegalencephaly patients who had received more than two preoperative MR examinations and the affected areas began to shrink in four out of the 12 patients. One of these four patients had diffuse hemimegalencephaly, and three had localized megalencephaly. In these atypical localized megalencephaly cases (Figs. 5 and 6), it was sometimes difficult to distinguish follow-up postatrophic MR findings from the differential diagnoses, such as multilobar cortical dysplasia. Various extracerebral abnormalities occurring outside of the involved hemisphere were very helpful in diagnosing localized megalencephaly. Sato et al. have reported that extracerebral abnormalities such as ipsilateral olfactory nerve enlargement, cerebral vascular dilatations, cerebellar enlargement, and abnormal architectures of bilateral or ipsilateral cerebellar folia are often associated with hemimegalencephaly [17]. In our study, extracerebral abnormalities were less frequently observed in the localized megalencephaly group than in patients with diffuse hemimegalencephaly. These extracerebral abnormalities seemed to correlate with the extent of the affected lesion of the hemimegalencephaly. Moreover, none of the extracerebral abnormalities were noted in patients with multilobar cortical dysplasia. These results can provide important clues for differentiating localized megalencephaly from multilobar cortical dysplasia.

A limitation of our study is that, since the two hospitals involved specialize in neurological care, patients were referred for the purpose of assessing operative indications. Therefore, more severe patients may have been selected compared to the usual population. Furthermore, although this study had the largest number of hemimegalencephaly patients of all previously reported studies, if more patients were involved and observed for a longer period, the clinical differences and outcomes among the three groups would be clearer.

Conclusion

We revealed that localized megalencephaly accounted for one quarter of all hemimegalencephaly cases. The incidence of extracerebral abnormalities in patients with localized hemimegalencephaly was almost half that of patients with diffuse hemimegalencephaly, although extracerebral abnormalities were absent in patients with multilobar cortical dysplasia. Associated extracerebral abnormalities may correlate with the extent of the affected lesion of the hemimegalencephaly and could provide an important clue for differentiating localized megalencephaly from multilobar cortical dysplasia.

Conflict of interest statement We declare that we have no conflict of interest.

References

1. Woo CL, Chuang SH, Becker LE, Jay V, Otsubo H, Rutka JT, Snead OC 3rd (2001) Radiologic–pathologic correlation in focal cortical dysplasia and hemimegalencephaly in 18 children. Pediatr Neurol 25:295–303
2. Yu J, Baybis M, Lee A, McKhann G 2nd, Chugani D, Kupsky WJ, Aronica E, Crino PB (2005) Targeted gene expression analysis in hemimegalencephaly: activation of beta-catenin signaling. Brain Pathol 15:179–186
3. Sato N, Ota M, Yagishita A, Miki Y, Takahashi T, Adachi Y, Nakata Y, Sugai K, Sasaki M (2008) Aberrant midsagittal fiber tracts in patients with hemimegalencephaly. AJNR Am J Neuroradiol 29:823–827
4. Fitz CR, Harwood-Nash DC, Boldt DW (1978) The radiographic features of unilateral megalencephaly. Neuroradiology 15:145–148
5. Renowden SA, Squier M (1994) Unusual magnetic resonance and neuropathological findings in hemimegalencephaly: report of a case following hemispherectomy. Dev Med Child Neurol 36:357–361
6. Manz HJ, Phillips TM, Rowden G, McCullough DC (1979) Unilateral megalencephaly, cerebral cortical dysplasia, neuronal hypertrophy, and heterotopia: cytomorphometric, fluorometric cytochemical, and biochemical analyses. Acta Neuropathol 15:97–103
7. Bosman C, Boldrini R, Dimitri L, Di Rocco C, Corsi A (1996) Hemimegalencephaly. Histological, immunohistochemical, ultrastructural and cytofluorimetric study of six patients. Childs Nerv Syst 12:765–775
8. Flores-Sarnat L (2002) Hemimegalencephaly: part 1. Genetic, clinical, and imaging aspects. J Child Neurol 17:373–384
9. King M, Stephenson JB, Ziervogel M, Doyle D, Galbraith S (1985) Hemimegalencephaly—a case for hemispherectomy? Neuropediatrics 16:46–55
10. Crino PB (2004) Malformations of cortical development: molecular pathogenesis and experimental strategies. Adv Exp Med Biol 548:175–191
11. De Rosa MJ, Secor DL, Barsom M, Fisher RS, Vinters HV (1992) Neuropathologic findings in surgically treated hemimegalencephaly: immunohistochemical, morphometric, and ultrastructural study. Acta Neuropathol 84:250–260
12. Vinters HV, Fisher RS, Cornford ME, Mah V, Secor DL, De Rosa MJ, Comair YG, Peacock WJ, Shields WD (1992) Morphological substrates of infantile spasms: studies based on surgically resected cerebral tissue. Childs Nerv Syst 8:8–17

13. Arai Y, Edwards V, Becker LE (1999) A comparison of cell phenotypes in hemimegalencephaly and tuberous sclerosis. Acta Neuropathol 98:407–413
14. Hoffmann KT, Amthauer H, Liebig T, Hosten N, Etou A, Lehmann TN, Farahati J, Felix R (2000) MRI and ^{18}F-fluorodeoxyglucose positron emission tomography in hemimegalencephaly. Neuroradiology 42:749–752
15. Salamon N, Andres M, Chute DJ, Nguyen ST, Chang JW, Huynh MN, Chandra PS, Andre VM, Cepeda C, Levine MS, Leite JP, Neder L, Vinters HV, Mathern GW (2006) Contralateral hemimicrencephaly and clinical–pathological correlations in children with hemimegalencephaly. Brain 129 (Pt 2):352–365
16. Kato M, Mizuguchi M, Sakuta R, Takashima S (1996) Hypertrophy of the cerebral white matter in hemimegalencephaly. Pediatr Neurol 14:335–338
17. Sato N, Yagishita A, Oba H, Miki Y, Nakata Y, Yamashita F, Nemoto K, Sugai K, Sasaki M (2007) Hemimegalencephaly: a study of abnormalities occurring outside of the involved hemisphere. AJNR Am J Neuroradiol 28:678–682
18. Barkovich AJ (2005) Pediatric neuroimaging. Lippincott Williams & Wilkin, Philadelphia, pp 337–341
19. D'Agostino MD, Bastos A, Piras C, Bernasconi A, Grisar T, Tsur VG, Snipes J, Juhasz C, Chugani H, Guerrini R, Cross H, Andermann E, Dubeau F, Montes J, Olivier A, Andermann F (2004) Posterior quadrantic dysplasia or hemi-hemimegalencephaly: a characteristic brain malformation. Neurology 62:2214–2220
20. Griffiths PD, Gardner SA, Smith M, Rittey C, Powell T (1998) Hemimegalencephaly and focal megalencephaly in tuberous sclerosis complex. AJNR Am J Neuroradiol 19:1935–1938
21. Riikonen R (2005) The latest on infantile spasms. Curr Opin Neurol 18:91–95
22. Barkovich AJ, Chuang SH (1990) Unilateral megalencephaly: correlation of MR imaging and pathologic characteristics. AJNR Am J Neuroradiol 11:523–531
23. Kalifa GL, Chiron C, Sellier N, Demange P, Ponsot G, Lalande G, Robain O (1987) Hemimegalencephaly: MR imaging in five children. Radiology 165:29–33
24. Wolpert SM, Cohen A, Libenson MH (1994) Hemimegalencephaly: a longitudinal MR study. AJNR Am J Neuroradiol 15:1479–1482